# Gas permeability of porous silicon nanostructures

V. Lysenko, J. Vitiello, B. Remaki, and D. Barbier
*Materials Physics Laboratory (LPM), CNRS UMR-5511, INSA de Lyon, 7 avenue Jean Capelle, Batiment Blaise Pascal, 69621 Villeurbanne Cedex, France*
(Received 20 January 2004; published 1 July 2004)

The gas (air and hydrogen) flow through porous silicon (PS) nanostructures is studied. Being well described by Darcy's law, the gas flow measurements allow us to deduce PS permeability values, which are measured to be $10^{-16}$–$10^{-15}$ $m^2$, corresponding to the 50–70% porosity range. A strong porosity dependence of the PS intrinsic permeability is found to be in good agreement with Kozeny's model. The influence of nanoscale morphology on the porous layer permeability is shown and discussed, taking into account the fractal-like specific surface of the PS nanostructures. In particular, the liquid permeability of the PS nanostructure is estimated to be $6.4\times10^{-18}$ $m^2$ from the observed Klinkenberg effect for gas flow.

DOI: 10.1103/PhysRevE.70.017301 PACS number(s): 47.55.Mh, 61.43.Gt, 47.15.−x

Because of its very large specific surface values (up to 1000 $m^2\,cm^{-3}$) [1], its high reactivity, and its potential compatibility with silicon-based electronics, porous silicon (PS) nanostructures are successfully used in gas sensing devices [2]. Recently, new gas-based applications of this type promised nanostructured material in miniaturized fuel cells [3] and gas precombustion microsystems [4] were reported. However, in spite of great interest to apply PS in such microsystems, gas transport in this porous material is not yet studied. In this work, we (i) describe gas flow through PS nanostructure, (ii) deduce porosity-dependent gas permeability of the PS nanostructures, and (iii) analyze, in detail, the permeability values in the frame of Kozeny's permeability model for porous media [5]. Weak physical interactions between flowing gases and nanoscale structural particularities of PS are observed.

The PS samples studied in this work were produced according to a standard procedure [6] of electrochemical etching of monocrystalline (100)-oriented boron-doped (0.01 Ω cm) Si wafers at current densities of 40–100 $mA\,cm^{-2}$. The etching solution was a 1:1 (by volume) mixture of ethanol and concentrated aqueous hydrofluoric acid (48%). Depending on current density, the porosity of the samples varied in the range of 50–70%. In order to obtain freestanding PS layers, a short (≈0.5–1 s) anodization current pulse of about 1 $A/cm^2$, ensuring an electropolishing regime, was applied at the end of the etching process. The thickness of the realized samples was about 100 $\mu$m. The dimension of Si nanocrystallites constituting the porous layer was estimated by Raman microspectroscopy, using a method described in detail elsewhere [7]. Some samples were slightly oxidized at low temperatures (<350 °C) in a dry $O_2$ atmosphere during 1 h to slightly modify the surface of the Si nanocrystallites by the creation of Si-O bonds.

To study gas flow through PS, the freestanding samples were mounted in a homemade hermetic cell. Air and hydrogen passed through the samples due to a pressure gradient maintained across the sample thickness. The different pressure gradients in the cell were hydrostatically established by the gas bubbling in a tube containing water columns of different heights. The outgoing gas flow rates were measured by a flowmeter.

The creeping flow of a single viscous fluid through a porous media is described by Darcy's law [5]

$$\vec{q} = -K\vec{\nabla}p, \tag{1}$$

which is a simple linear transport law having exactly the same form as Ohm's law, Fick's law, and the heat conduction equation, and where $\vec{q}$ is the flux of the fluid through the porous media, $\vec{\nabla}p$ is the pressure gradient of the fluid across the porous media, and the coefficient of proportionality $K$ is the conventional saturated permeability characterizing fluid conductivity through the porous media. We note that the permeability so defined depends both on the porous media and on the fluid, and varies inversely as the fluid viscosity, $\mu$. We can, therefore, define an intrinsic permeability, $k=K\mu$, which is the porous media property, independent of the fluid used to measure it.

The prediction of the permeability for various porous media is a problem of great practical relevance. In general, some functional correlations between the permeability and other macroscopic properties of the porous media, such as porosity (ratio of the total void volume) $P$ and specific surface area (total interstitial surface area to the bulk volume) $S$, can be established. One of the most known correlations is based on the simple capillary theory of Kozeny [5]. Within the model, the intrinsic permeability is given as [5]

$$k = \frac{P^3}{c\tau^2 S^2}, \tag{2}$$

where $c$ is the Kozeny coefficient that depends on the geometry of the capillaries ($c=2$ for cylindrical capillaries) and $\tau$ is the turtuosity of the porous medium [8].

While considering gas flow through a porous medium, only the interconnected pores going from one side to another of the porous sample participate in the gas conduction, as the dead-end pores almost do not contribute to the flow forming the nonconducting pore space of the medium. Therefore, to include the effect of the dead-end pores, the total geometrical porosity, $P$, is replaced in Eq. (2) by effective porosity, $P_{eff}$, defined as the ratio of the volume of the only conducting pores to the total porous sample volume. For high porous

 

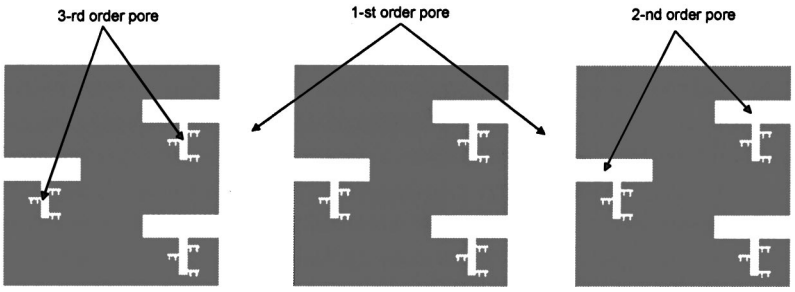


FIG. 1. A schematic view of the freestanding fractal-like porous silicon nanostructure.

materials, the effective porosity $P_{eff}$ should approach the geometrical one, $P$, and for low porous samples $P_{eff} < P$, and it has to be taken into account for realistic permeability prediction.

PS is considered as a fractal-like porous nanostructure that seems to be close to the nanopores networks observed by electronic microscopy [9]. It is schematically shown in Fig. 1. The largest first-order pores produce perpendicular pores with proportionally smaller sizes, each of them generating the next perpendicular branches and so on. In such a "low porosity" presentation (Fig. 1), only the first-order pores are evident to contribute in the gas flow ($P_{eff} < P$). For higher porosities, the pores of the higher order become interconnected, and $P_{eff}$ begins to approach $P$ and finishes to be very close to $P$.

Figure 2(a) shows an example of gas flow rates for hydrogen and air as a function of the maintained pressure gradient for a given PS nanostructure. An ideal linear behavior in accordance with the Darcy law given by Eq. (1) can be observed. The gas-dependent permeability, $K$, of PS can be therefore obtained from the line slope. Strong nonlinear porosity dependence of the permeability so deduced is given in Fig. 2(b). The permeability to hydrogen is observed to be much larger than that to air, due to an important difference in their viscosity (28.6 $\mu$Pa s for air and 9 $\mu$Pas for hydrogen). However, from a physical point of view, the understanding of the porosity-dependent behavior of intrinsic (gas independent) permeability, $k = K\mu$, of the PS nanostructures, obtained by excluding the gas viscosity, is more important.

Figure 3 shows the intrinsic permeability versus porosity. In the first-order approximation, the PS permeability values obtained with air and hydrogen are quite close, indicating independence on gas nature. The experimental points can be quite well fitted by Kozeny's model [Eq. (2)]. Indeed, using Eq. (2) and taking into account the theoretical porosity dependence of the PS specific surface $S = 6(1-P)/d$, which is in good agreement with experimental values [1], and where $d$ is the mean dimension of the Si nanocrystallites, the experimental results are fitted (solid line in Fig. 3) by the following relation:

$$k = A\frac{P_{eff}^3}{\tau^2(1-P)^2}, \tag{3}$$

where $P_{eff}$ and $\tau$ are expressed in the same manner as proposed by Koponen *et al.* for another porous medium [5,8]

$$P_{eff} = 0.3x^3 - 0.93x^2 + 1.63x, \quad \text{with} \quad x = (P - 0.33)/0.67, \tag{4}$$

$$\tau = 0.8(1-P) + 1, \tag{5}$$

$k$ is the intrinsic permeability in ($m^2$) and $A$ is the fitting coefficient equal to $5.5 \times 10^{-16}$ ($m^2$). The coefficient $A$ is expressed as: $A = d^2/36c$, where $c$ is a geometrical (shape) parameter of Kozeny's model [Eq. (2)]. Neglecting the weak porosity dependence of the nanocrystallite dimension, $d$, and taking its mean value of 16 nm for this porosity range (see the insert in Fig. 3), we obtain $c \approx 0.014$, which is character-

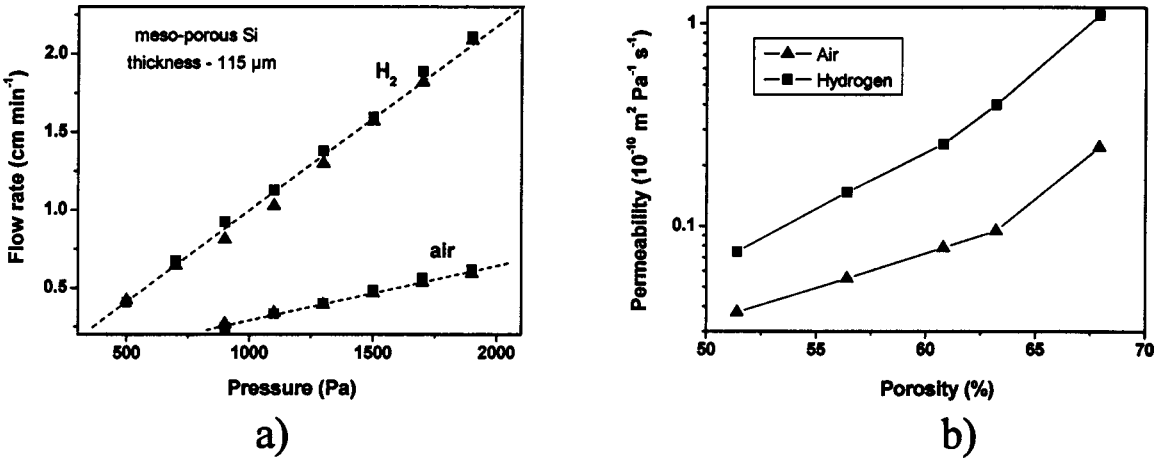


FIG. 2. (a) The rates of hydrogen and air flows through the freestanding porous silicon layers as functions of applied pressure. The squared and triangular symbols correspond to two independent consequent measurements in order to check repeatability. (b) The permeability of porous silicon nanostructures to hydrogen and air as functions of the layer porosity.

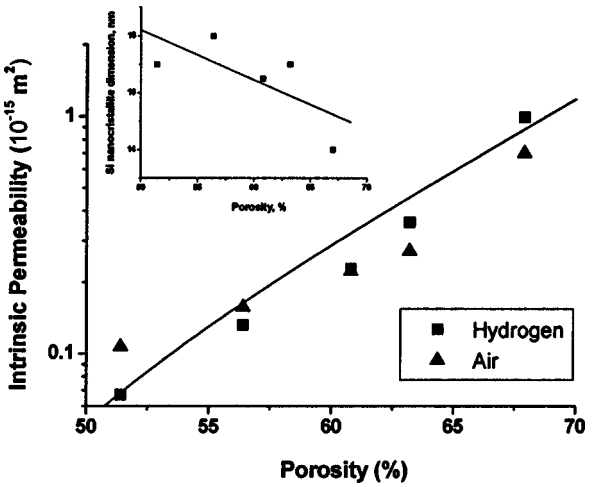


FIG. 3. The intrinsic (theoretically gas independent) permeability of the porous silicon as a function of porosity. The data are fitted according to Kozeny's law (solid line). The insert (upper left corner) shows dimensions (for the same porosity range) of the silicon nanocrystallites constituting the porous layer.

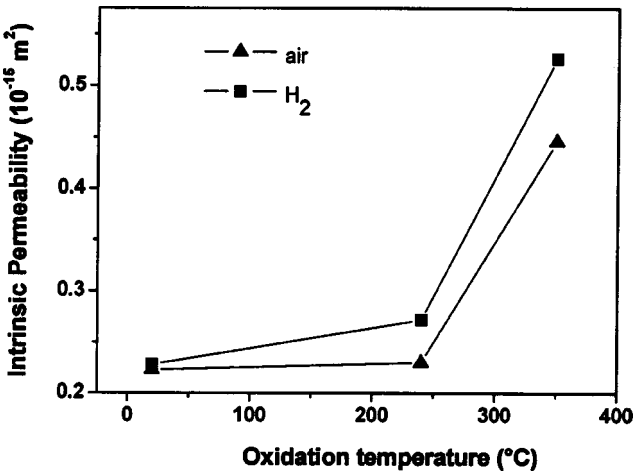


FIG. 4. The influence of low temperature oxidation on gas permeability of the porous silicon nanostructures.

istic for our randomly arranged PS nanostructure, and completely different from the case of strongly cylindrical pores [5] characterized by $c=2$. In our minds, such a difference between our empirically deduced value of the shape parameter $c$, and that used for the case of the regular cylindrical pores reflects a structural complexity at the nanoscale level of the PS morphology. Indeed, (i) strong percolation of the nanopores, (ii) statistical and in-space distribution of their dimensions and complex shapes, and (iii) the fractal nature of the whole porous network and of the structural irregularities at nano- and subnanoscale levels determine, in our opinion, the observed difference.

However, a more careful observation of the experimental results (Fig. 3) reveals a weak dependence of the permeability values on the nature of gas molecules. Indeed, one can see that the PS permeability increase, along with the porosity, is slightly steeper when hydrogen is used as a testing gas, rather than air. It can be explained by the Klinkenberg effect [10], originally detected with gas flow through capillary tubes. Indeed, this effect is well pronounced when the diameter of the capillary tubes approaches the mean-free path ($\Lambda$) of the gas molecule. For a majority of gasses at normal conditions, the mean-free path is well known to be about 100 nm, which is much larger than the characteristic pore diameter in PS($\approx$6–8 nm [11]). Thus, in PS nanostructures, numerous scattering events take place between gas molecules and nanopore walls. Consequently, the pore diameter can be thus considered, in a first-order approximation, as an effective mean-free path ($\Lambda_{eff}$) for gas molecules traveling through the porous medium. However, for equal pressures and a given porosity, smaller and lighter hydrogen molecules will be less scattered (larger mean-free path) than larger air molecules (smaller mean-free path) when traveling through the same PS nanostructure. When the porosity increases, the mean-free path for hydrogen molecules should increase more rapidly than for air molecules. Being related to $\Lambda_{eff}$ as [12] $k \sim \Lambda_{eff}^2$, the permeability dependence on the porosity should be, therefore, steeper for hydrogen than for air, which is correlated to the obtained results (Fig. 3).

Taking an average value of the measured intrinsic permeability corresponding to 67% porosity $k_a \approx 5 \times 10^{-16}$ m$^2$, an average value of applied pressures: $p_a \approx 1300$ Pa, a Klinkenberg factor $b$, corresponding to the $k_a$ value [10] $b \approx 10^5$ Pa and the following relation [10]:

$$k_a = k_\infty \left(1 + \frac{b}{p_a}\right), \tag{6}$$

we estimate an absolute (gas independent) permeability, $k_\infty$, under the very large gas-phase pressure at which condition the Klinkenberg effects are negligible to be about $6.4 \times 10^{-18}$ m$^2$. A gas is compressed into a liquidlike state at $p_a \to \infty$, and $k_\infty$ corresponds, therefore, to the permeability of a liquid that completely fills the nanopores of the PS.

In spite of the larger mean-free path due to the Klinkenberg effect, absolute $k$ values are observed to be smaller, in the case of hydrogen, for a low porosity range ($P<60\%$). It can be explained by a possible physical trapping of gas molecules in nonconducting dead-end pores (the pores of a high order in Fig. 1). Being lighter and smaller, hydrogen is thus more probable to be trapped, and the corresponding apparent PS permeabilities should be smaller than for air. For $P>60\%$, the trapping effects are less present, both due to the much larger $\Lambda_{eff}$ and due to the traps' disappearance when $P_{eff} \to P$ and $k$ values measured with hydrogen molecules become, therefore, larger than those estimated by means of air flow. In this porosity range ($P>60\%$), only the Klinkenberg effect dominates. Let us insist, however, that the discussed Klinkenberg and trapping effects are relatively weak, and the porosity-dependent permeability behavior is relatively well described by Kozeny's model, independent of the gas nature.

The existence of the trapping effect is unambiguously demonstrated in Fig. 4. A slight (low temperature: $<350$ °C) oxidation of the freestanding PS samples was performed. Such a treatment results, surprisingly, in an enhancement of the PS intrinsic permeability. Indeed, after the oxidation,

smaller (higher-order) dead-end pores are partially or completely plugged, leading to the partial trap's disappearance, while the larger (lower-order) interconnected gas conductive porous network, corresponding to the $P_{eff}$, is preserved unchanged. This effect is more pronounced for hydrogen as lighter and smaller molecules, compared to air and, therefore, is more sensible to the traps' presence/absence. In particular, after the first oxidation step corresponding to 240 °C, hydrogen permeability increases while the air permeability remains at the same level. It can be explained by the plugging of the smallest pores trapping only hydrogen, while the oxidation at 350 °C leads to the removing of the larger trapping pores, where both hydrogen and air molecules could be enclosed, and consequently, the permeabilities both to air and to hydrogen are enhanced. It is important to make that precise during the slight oxidation procedure at such low temperatures, so that no destruction occurs of the initial as-prepared porous network, which could provoke the permeability enhancement. Indeed, as it is well known from a technological point of view, the oxidation of PS at 300 °C in a dry $O_2$ atmosphere is used for the stabilization of the PS physical properties. The oxidized fraction of silicon atoms is usually smaller than 20–25% when the oxidation temperatures do not exceed 350 °C. Taking into account that 20–30% of the silicon atoms are found at the PS specific surface, one can conclude that only a monolayer (on average) of silicon oxide can be formed at the silicon nanocrystallites surfaces at temperatures $<350$ °C and it is evident to be not sufficient for the mechanical destruction of the whole PS layer.

In conclusion, the gas permeability of nanostructured PS is studied. Gas transport through the PS freestanding layers can be well described by Darcy's law, as for other porous media. The PS intrinsic permeability dependence on porosity is in good agreement with Kozeny's model. A weak permeability dependence on the nature of the used gas molecules is observed and explained by random physical interactions (Klinkenberg and trapping effects) between the traveling gas molecules and PS nanoscale morphology.

The authors are grateful to J.-Y. Laurent and C. Roux from the Departement of Technologies for New Energies (DTEN) of the Grenoble Atomic Energy Centre (CEA) for assistance in permeability measurements.

[1] R. Herino, in *Properties of Porous Silicon*, edited by L. T. Canham (INSPEC/IEE, London, 1997), p. 89, and references therein.
[2] G. Barillaro, A. Nannini, and F. Pieri, Sens. Actuators B **93**, 263 (2003), and references therein.
[3] See, for example, J. P. Meyers and H. L. Maynard, J. Power Sources **109**, 76 (2002).
[4] A. Splinter, J. Stürmann, O. Bartels, and W. Benecke, Sens. Actuators B **83**, 169 (2002).
[5] A. Koponen, M. Kataja, and J. Timonen, Phys. Rev. E **56**, 3319 (1997).
[6] A. Halimaoui, in *Properties of Porous Silicon*, edited by L. T. Canham (INSPEC/IEE, London, 1997), p. 12.
[7] See, for example, H. Campbell and Ph. M. Fauchet, Solid State Commun. **58**, 739 (1986).
[8] A. Koponen, M. Kataja, and J. Timonen, Phys. Rev. E **54**, 406 (1996).
[9] M. Wesolowski, Phys. Rev. B **66**, 205207 (2002), and references therein.
[10] Y-S. Wu, K. Pruess, and P. Persoff, Transp. Porous Media **32**, 117 (1998).
[11] R. Herino, G. Bomchil, K. Barla, C. Bertrand, and J. L. Ginoux, J. Electrochem. Soc. **134**, 1994 (1987).
[12] S. Mauran, L. Rigaud, and O. Coudevylle, Transp. Porous Media **43**, 355 (2001).